Marine Pollution Bulletin 166 (2021) 112248

Contents lists available at ScienceDirect

Marine Pollution Bulletin

journal homepage: www.elsevier.com/locate/marpolbul

PAH source differentiation between historical MGP and significant urban influences for sediments in San Francisco Bay

Randy E. Jordan [a,*], Mark J. Cejas [b], Helder J. Costa [c], Theodor C. Sauer Jr [d], Laura S. McWilliams [e]

[a] Natural Spectrum LLC, 1782 Bungalow Way NE, Poulsbo, WA 98370, USA
[b] ChemQuants LLC, 414 Olive St., Santa Barbara, CA 93101, USA
[c] Haley & Aldrich, Inc., 2033 N. Main Street, Suite 309, Walnut Creek, CA 94596, USA
[d] P.O. Box 2652, Duxbury, MA 02331, USA
[e] Haley & Aldrich, Inc., 5333 Mission Center Rd., Suite 300, San Diego, CA 92108, USA

ARTICLE INFO

Keywords:
PAH diagnostic ratios
PVA
MGP
Sediment

ABSTRACT

A forensic source evaluation of polycyclic aromatic hydrocarbons (PAHs) in nearshore sediments in San Francisco Bay examined total PAH greater than ambient concentrations in sediments, and potential pyrogenic source relationships with respect to PAH compounds typically associated with point and nonpoint pyrogenic source types, including PAHs potentially associated with historical manufactured gas plant (MGP) operations. Diagnostic source ratio analysis was employed for determination of potential PAH source relationships. A two-model approach indicated distinct potential source signatures, as identified from the distributions of higher PAH concentrations in some sediments. Source characterization was aided by Polytopic Vector Analysis (PVA) and data visualization with t-Distributed Stochastic Neighbor Embedding (t-SNE). Two signatures exhibited pyrogenic character likely consistent with historical MGP sources, and one signature was related to creosote. A distinct and significant source of PAHs to the investigation area sediment consisted of ubiquitous nonpoint and potential unidentified point sources is termed "urban influence".

1. Introduction

A forensic evaluation was undertaken to determine potential sources of polycyclic aromatic hydrocarbons (PAHs) in nearshore sediments in a waterfront portion of San Francisco Bay, California. The forensic analysis considered sediment sample data generated from multiple sampling events during 2016–2018 for 154 station locations in San Francisco (Haley & Aldrich, 2017, 2018a), as shown in Fig. 1. Additional information included data from creosote-treated timber pile samples collected from the San Francisco waterfront. Comprehensive source evaluation using diagnostic source ratio analysis was aided with a multivariate analysis approach, using Polytopic Vector Analysis (PVA) for data exploration and t-Distributed Stochastic Neighbor Embedding (t-SNE) for data visualization.

The evaluation considered PAH composition in sediments with total PAH concentrations above "ambient" conditions relative to the San Francisco Estuary Institute (SFEI) Regional Monitoring Program (RMP) list of 25 PAHs (SFEI, 2016), as shown in Table 1. The RMP has defined the Central San Francisco Bay "ambient" concentration of total PAHs as 4.5 mg/kg, based on the sum of the RMP list of 25 PAHs, hereinafter referred to as "TPAH". Table 1 also lists other parent and alkylated PAHs and other hydrocarbons of interest to this evaluation.

The forensic study objectives included the following:

- Identify sources of high TPAH (i.e., significantly greater than "ambient") concentrations to sediment samples, which may represent historical and/or ongoing point sources.
- Identify distinct compositional features, using both PAH diagnostic ratios and multivariate analysis, that could serve to: define potential source signatures in the sediments; differentiate potential point and nonpoint petrogenic and pyrogenic source types; and identify PAHs potentially associated with manufactured gas plant (MGP) operations due to the historical presence of MGP facilities in the vicinity.

* Corresponding author.
E-mail addresses: rjordan@natural-spectrum.com (R.E. Jordan), markcejas@chemquants.com (M.J. Cejas), hcosta@haleyaldrich.com (H.J. Costa), tsauer@haleyaldrich.com (T.C. Sauer), lmcwilliams@haleyaldrich.com (L.S. McWilliams).

https://doi.org/10.1016/j.marpolbul.2021.112248
Received 9 December 2020; Received in revised form 25 February 2021; Accepted 4 March 2021
Available online 15 March 2021

- Identify potential "urban influence" reflecting a combination of nonpoint and unidentified point sources, which may be distinguished from identified high-concentration point source signatures.

A previous sediment study of six station locations within the Pier 39 marina with focus on MGP-related residues also suggested the presence of other non-MGP pyrogenic PAH sources. The forensic evaluations characterized the sediment as containing MGP-related residues commingled with anthropogenic hydrocarbons, presumably from urban runoff and/or atmospheric deposition (NewFields, 2015).

2. Methods

2.1. Sample analysis

PAH analytical results were compiled from a total of 980 surface and subsurface sediment samples from multiple sampling events conducted from July 2016 to April 2018. Surface sediments were taken from 154 station locations as grab samples and shallow subsurface sediment push core sections, all taken 0–0.5 ft. below sediment surface. Deeper subsurface sediment samples were generally from one-foot intervals for core depths of 0.5 ft. to about 20 ft. below sediment surface (Haley & Aldrich, 2017). The forensic evaluation considered data for surface and subsurface sediments. Sediment samples were analyzed for a comprehensive suite of PAHs (Table 1) by Alpha Analytical (Mansfield, Massachusetts) using a modification of U.S. EPA Method 8270D, gas chromatography/mass spectrometry (GC/MS) with selected ion monitoring (SIM). Laboratory Data Consultants performed data validation of PAH GC/MS-SIM results.

The evaluation also included data from six creosote timber pile samples collected by NewFields on behalf of the Port of San Francisco. The wood pile samples were analyzed by the same laboratory and methods as the sediment samples.

2.2. Multivariate data analysis

The multivariate analysis approach, using PVA for data exploration and t-SNE for data visualization, defined end-members as PVA-based mathematical constructions to be used in the characterization of actual sample PAH compositions based on sample analysis data. The integrated application of PVA and t-SNE has been employed for chemometric evaluations of complex environmental systems involving multiple contaminant sources (Cejas and Barrick, 2021).

The data set for multivariate statistics was reduced to focus on the more recalcitrant 4–6 ring PAHs that are more relevant for studies of MGP-related residuals and other pyrogenic sources. Detection limits for undetected PAHs were not censored (i.e., MDL values were used) due to the low percentage of non-detects in the data set and the fact that all of the samples were processed and analyzed in the same laboratory. After data reduction the data matrix was range transformed after row-sum normalization (Miesch, 1976) to homogenize the variance among all variables and minimize the influence of those with substantial means. The transformation technique also reduced concentration-dependent skewness of higher-concentration analytes.

The EXTENDED QMODEL version of PVA was utilized to assess PAH compositions in the sediments (Full et al., 1981; Ehrlich et al., 1994). The software used is a collection of MATLAB scripts developed by Dr. Glenn Johnson. Two techniques were applied to appraise the reduced dimensional structure of the data set, and for the end-member determination of the PVA model: 1) Coefficient of Determination (CD) variable diagnostics; and 2) Varimax loadings index. CD variable diagnostics is a criterion used to assess the quality of the PVA model by testing if the

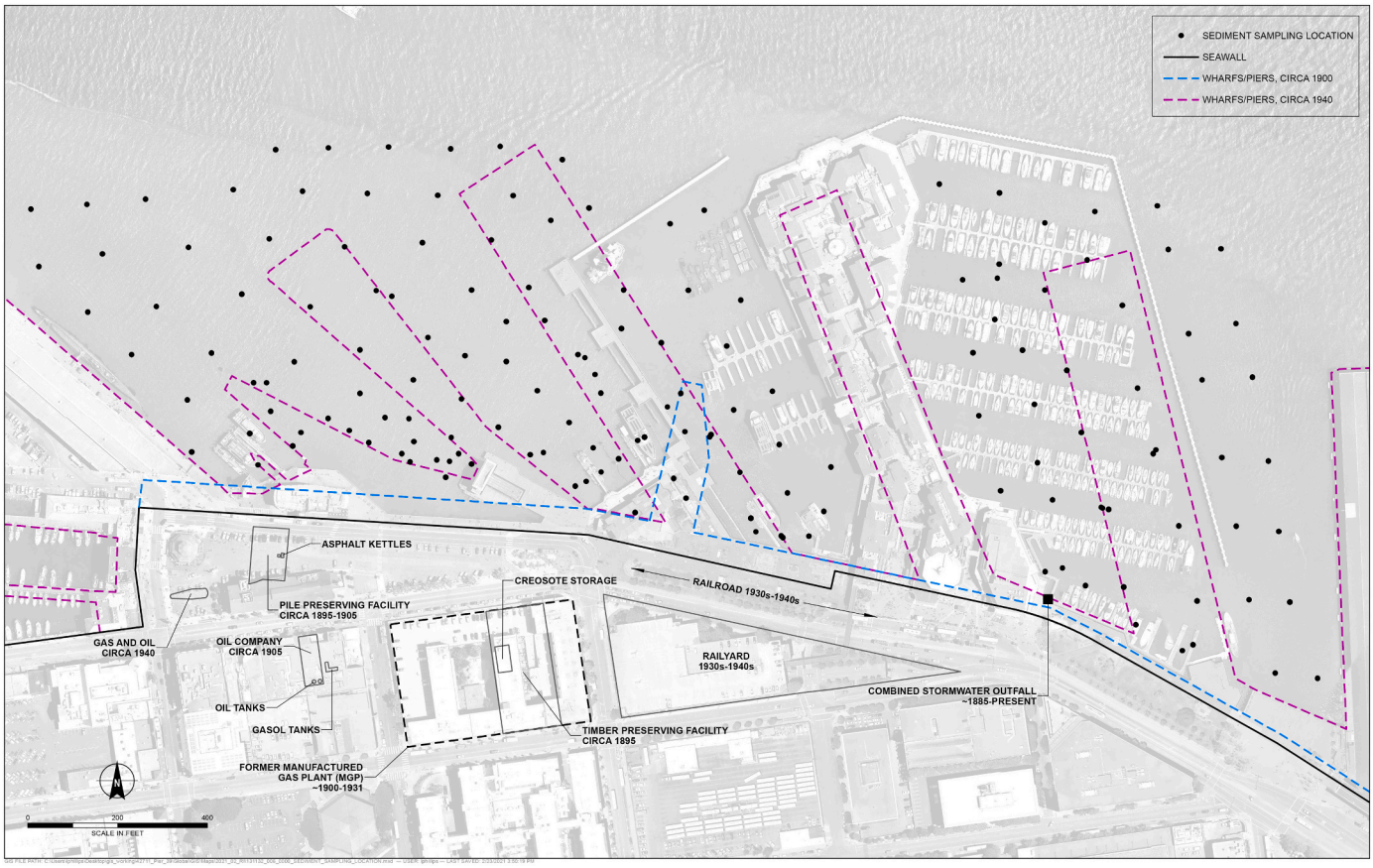

Fig. 1. Sediment sampling station locations, San Francisco Bay, California.

Table 1
Decalins and PAHs evaluated and compounds designated as San Francisco Estuary Institute Regional Monitoring Program PAHs.

Compound name	
Decalin (D0)	Fluoranthene (FL0)[a]
C1-Decalins (D1)	Pyrene (PY0)[a]
C2-Decalins (D2)	C1-Fluoranthenes+Pyrenes (FP1)
C3-Decalins (D3)	C2-Fluoranthenes+Pyrenes (FP2)
C4-Decalins (D4)	C3-Fluoranthenes+Pyrenes (FP3)
Benzothiophene (BT0)	C4-Fluoranthenes+Pyrenes (FP4)
C1-Benzo(*b*)thiophenes (BT1)	Naphthobenzothiophenes (NBT0)
C2-Benzo(*b*)thiophenes (BT2)	C1-Naphthobenzothiophenes (NBT1)
C3-Benzo(*b*)thiophenes (BT3)	C2-Naphthobenzothiophenes (NBT2)
C4-Benzo(*b*)thiophenes (BT4)	C3-Naphthobenzothiophenes (NBT3)
Naphthalene (N0)[a]	C4-Naphthobenzothiophenes (NBT4)
C1-Naphthalenes (N1)	Benz(*a*)anthracene (BA0)[a]
C2-Naphthalenes (N2)	Chrysene (C0)[a]
C3-Naphthalenes (N3)	C1-Chrysenes (BC1)
C4-Naphthalenes (N4)	C2-Chrysenes (BC2)
Biphenyl (B)[a]	C3-Chrysenes (BC3)
Acenaphthylene (ACY)[a]	C4-Chrysenes (BC4)
Acenaphthene (ACE)[a]	Benzo(*b*)fluoranthene (BBF)[a]
Dibenzofuran (DF)	Benzo(*j*)fluoranthene (BJF)
Fluorene (F0)[a]	Benzo(*k*)fluoranthene (BKF)[a,b]
C1-Fluorenes (F1)	Benzo(b + k)fluoranthene (BBKF)[c]
C2-Fluorenes (F2)	Benzo(*a*)fluoranthene (BAF)
C3-Fluorenes (F3)	Benzo(*e*)pyrene (BEP)[a]
Dibenzothiophene (DBT0)[a]	Benzo(*a*)pyrene (BAP)[a]
C1-Dibenzothiophenes (DBT1)	Perylene (PER)[a]
C2-Dibenzothiophenes (DBT2)	Indeno(1,2,3-c,d)pyrene (IND)[a]
C3-Dibenzothiophenes (DBT3)	Dibenz(*a*,*h*)anthracene (DA)[a]
C4-Dibenzothiophenes (DBT4)	Benzo(*g*,*h*,*i*)perylene (GHI)[a]
Anthracene (A0)[a]	1-Methylnaphthalene[a]
Phenanthrene (P0)[a]	2-Methylnaphthalene[a]
C1-Phenanthraenes+Anthracenes (P1)	2,6-Dimethylnaphthalene[a]
C2-Phenanthraenes+Anthracenes (P2)	2,3,5-Trimethylnaphthalene[a]
C3-Phenanthraenes+Anthracenes (P3)	1-Methylphenanthrene[a]
C4-Phenanthraenes+Anthracenes (P4)	

[a] RMP PAH (SFEI, 2016).
[b] Reported by analytical lab and plotted herein as benzo(j + k)fluoranthene (BJKF).
[c] Diagnostic PAH ratio cross-plots show BBKF, as sum of benzo(*b*)fluoranthene + benzo(j + k)fluoranthene.

original variable data space can be reconstituted from the reduced eigenvector model data space. Ehrlich et al. (1994) concluded that those variables with CDs less than 0.5 typically provide little support to the PVA model. The Varimax loading index is the count of samples with high loadings >0.1 on a particular eigenvector.

By these criteria, a significant end-member has high loading (>0.1) for a majority of eigenvectors samples. Although end-members with a small percentage of high loading samples (>0.1) per eigenvector can be important as well, and represent a sample from a population that is not adequately represented in the data set. Factors one to five of the PVA model had loadings with a Varimax index >0.1 for 0.98, 0.99, 0.40, 0.25, and 0.005 proportions of the data set, respectively. All variables in the five factor PVA model exhibited CDs > 0.61, with a maximum of 0.96, median of 0.92, and mean of 0.87.

The t-SNE is a non-parametric technique that is a variation of Stochastic Neighbor Embedding (van der Maaten and Hinton, 2008). The decision to integrate t-SNE into this chemical source investigation was driven by two objectives. First, to employ a data-visualization technique capable of dependably retaining the sizeable high-dimensional data attributes of the large sample data set in an interpretable 2-D coordinate system. Secondly, t-SNE provided a visually intuitive platform for PVA modeling.

3. Results and discussion

The following describes the approach, process, and results for defining potential PAH source signatures and the development of source models, using data for sediments with TPAH concentrations greater than 100 mg/kg. The TPAH concentration level of 100 mg/kg was assumed as reasonable to consider sediment samples with likely point source influence and minimize the influence of mixing with nonpoint source and minor unidentified point sources comprising urban influence. Also discussed is the application of the source models to sediments with TPAH concentrations that are lower than the 100 mg/kg TPAH concentration threshold used to presume point-source influence, but still greater than the Central San Francisco Bay ambient concentration. The comprehensive PAH source evaluation combined conventional PAH diagnostic source ratio analysis with multivariate analysis using PVA and t-SNE techniques.

The forensic approach involved a multi-step process with the sequential objectives for: (1) identifying potential MGP and creosote source signatures and defining a PAH diagnostic source ratio model(s); (2) applying the diagnostic source ratio model(s) to sediment samples in order to identify the presence of these signatures as well as unspecified point sources with combined nonpoint sources as urban influence; and (3) employing multivariate analysis using PVA and data evaluation with t-SNE mapping to identify statistically derived end-members and also determine additional PAH diagnostic ratios to further characterize potential pyrogenic point sources (MGP and creosote) and predominantly pyrogenic urban influence signatures.

3.1. Identification of Potential PAH Source Signatures and Diagnostic Ratio Source Models

The first step explored potential pyrogenic point source signatures, using specific PAH diagnostic ratios, to help determine the potential for MGP-related influence. Candidate PAHs and associated ratio pairs included those used in previous investigations related to MGP-related and other pyrogenic source types (EPRI, 2000; Yunker et al., 2002; Costa et al., 2004; Costa and Sauer, 2005). To be effective, the selected PAH ratios must be representative of the source material and retain their relative concentrations during the course of environmental weathering. The effects of environmental weathering and other degradative processes typically remove the prominent lower molecular weight PAHs, and the profiles of weathered MGP residues in sediments can be similar to those of sediment samples that reflect urban background, or nonpoint urban influence (Brenner et al., 2002; Costa et al., 2004; Costa and Sauer, 2005; Uhler and Emsbo-Mattingly, 2006). Cumulative weathering effects on the higher molecular weight PAH assemblages have not been shown to confound the ability to distinguish between pyrogenic and petrogenic sources, based on field and laboratory weathering studies (Boehm et al., 2018). The environmental stability of paired PAH ratios has been demonstrated for various weathered source materials, such as crude petroleum (Douglas et al., 1996), pyrogenic tars (Uhler and Emsbo-Mattingly, 2006), and creosote (Brenner et al., 2002).

Various PAH diagnostic ratio candidates were evaluated with emphasis on apparent distributions for sediment samples with TPAH concentrations greater than 100 mg/kg, with the goal of defining the most useful source model(s) for evaluating the potential presence of the identified source signatures in sediment samples with TPAH concentrations greater than 100 mg/kg. TPAH. The emphasis on samples with TPAH greater than 100 mg/kg allowed for more reliable point source assignments, while minimizing the potential reduction in the number of samples used to define potential end-members. This process included sediment data for all station locations and all sampling depths (surface and subsurface) with greater than 100 mg/kg TPAH by plotting TPAH versus each of the PAH diagnostic ratios. This helped to determine the utility of a particular diagnostic ratio for defining a potential PAH source (Costa and Sauer, 2005). The selected PAH diagnostic ratios could then be evaluated in pairs as cross-plots to help determine their utility for defining source signature attributes and also evaluating those signatures in sediment samples with TPAH concentrations less than 100 mg/kg. In this context, the selected cross-plots are hereinafter referred to as "PAH

source ratio models".

The PAH diagnostic ratios considered for this forensic study include: fluoranthene/pyrene, benzo(b + k)fluoranthene/benzo(*a*)pyrene, and C1-chrysenes/C1-fluoranthenes+pyrenes. The benzo(*b*)fluoranthene and benzo(*k*)fluoranthene isomers can be difficult to resolve during the chromatographic analysis, so forensic interpretation will often consider the combined isomers as benzo(b + k)fluoranthene, as is the case with data used in this evaluation. The environmental stability of these select PAH diagnostic ratios, in relation to their use as potential source indices in pyrogenic tars, has been evaluated with controlled studies of tar evaporation and aerobic degradation for simulated environmental weathering (Uhler and Emsbo-Mattingly, 2006). With respect to evaporative loss, stability was evident for the fluoranthene/pyrene and benzo (b + k)fluoranthene/benzo(*a*)pyrene ratios, but the C1-chrysenes/C1-fluoranthenes+pyrenes ratio showed greater variability. For these ratios, biodegradation influence was most apparent for fluoranthene/pyrene and C1-chrysenes/C1-fluoranthenes+pyrenes. In these studies, the fluoranthene/pyrene and C1-chrysenes/C1-fluoranthenes+pyrenes ratios decreased over the experimental timeframes for both weathering evaluations. Analysis of field samples from a former MGP site that had undergone varying degrees of weathering indicated that the fluoranthene/pyrene and benzo(b + k)fluoranthene/benzo(*a*)pyrene indices were stable, but the C1-chrysenes/C1-fluoranthenes+pyrenes ratio was more variable. These studies indicate that while fluoranthene/pyrene and benzo(b + k)fluoranthene/benzo(*a*)pyrene ratios were stable and should be considered as very suitable for source identifications, the apparent weathering-related variability must be taken into account when using the C1-chrysenes/C1-fluoranthenes+pyrenes ratio for this purpose. These controlled laboratory studies represent severe biodegradation and weathering potential relative to ambient conditions. Therefore, PAH ratio stability under laboratory conditions supports the use of these specific diagnostic source ratios in field samples.

Fig. 2 shows the distributions for each PAH diagnostic ratio relative to TPAH for high PAH concentration sediments from all sampling stations. The plot of TPAH versus fluoranthene/pyrene (Fig. 2a) appears to reveal multiple TPAH maxima relative to ranges of the fluoranthene/pyrene ratio, which is not as apparent for the plot of benzo(b + k)fluoranthene/benzo(*a*)pyrene (Fig. 2b). The representations for C1-chrysenes/C1-fluoranthenes+pyrenes (Fig. 2c) show a distribution with a possible concentration dependence. This source ratio plot does not reveal distinct maxima that would suggest multiple sources, perhaps reflecting mixing with combined nonpoint sources. It is critical to note that the trend towards higher ratio values (Fig. 2c) does not suggest a potential weathering effect, based on controlled experimental weathering studies that demonstrated decreasing ratios resulting from evaporative weathering and biodegradation (Uhler and Emsbo-Mattingly, 2006). The ratio pairs of benzo(b + k)fluoranthene/benzo(*a*)pyrene and C1-chrysenes/C1-fluoranthenes+pyrenes to fluoranthene/pyrene were selected for potential source characterization.

The cross-plots shown in Fig. 3 for sediments with high TPAH concentrations from all sampling stations suggest several possible clusters for both benzo(b + k)fluoranthene/benzo(*a*)pyrene versus fluoranthene/pyrene (Fig. 3a) and C1-chrysenes/C1-fluoranthenes+pyrenes versus fluoranthene/pyrene (Fig. 3b). These distributions suggest the possibility of multiple distinct high-concentration point sources, confirming the potential utility of these PAH diagnostic ratio pairs for helping to identify potential pyrogenic source signatures. Fig. 3 also shows the creosote pile samples, discussed below. The following

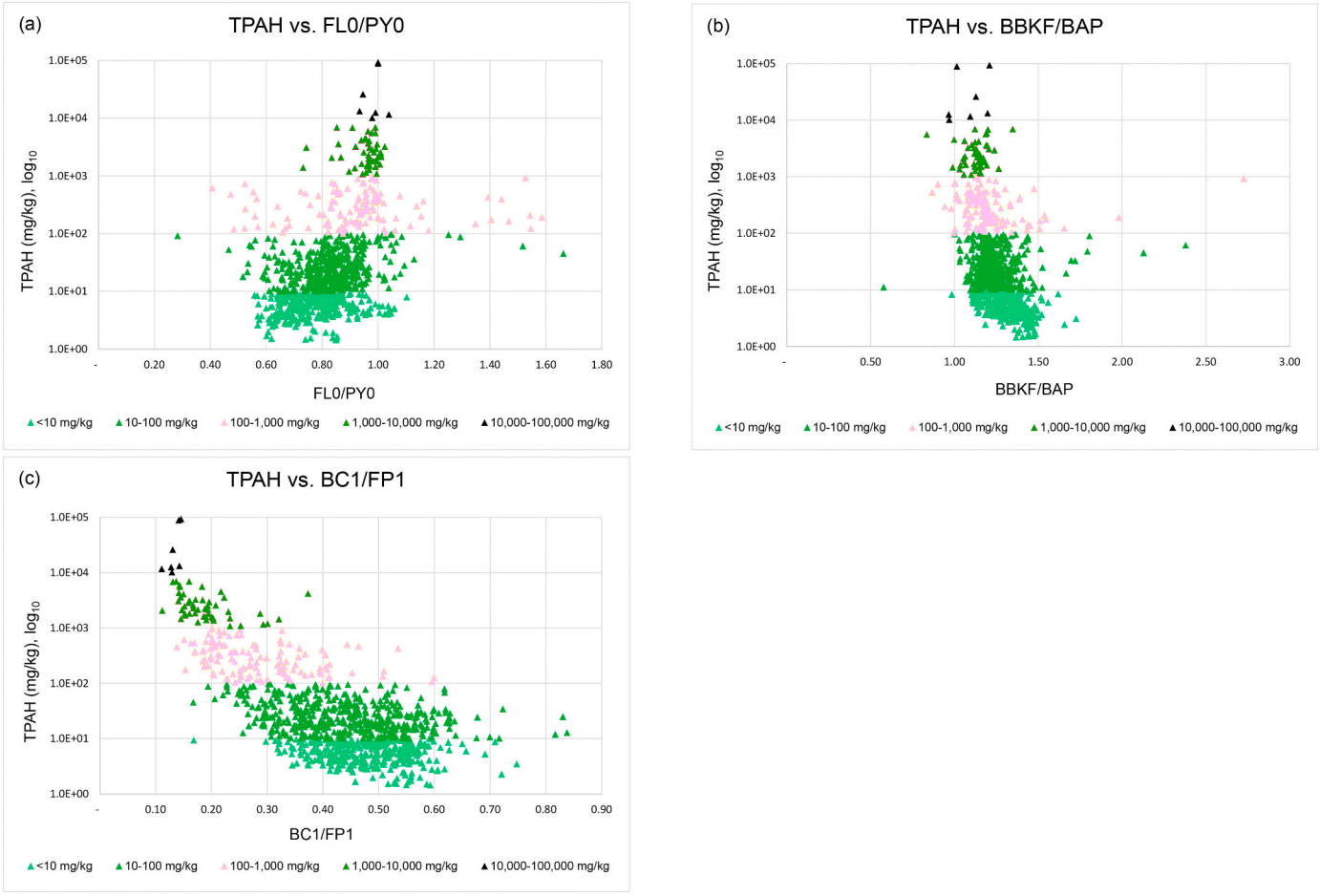

Fig. 2. Screening of potential PAH diagnostic ratios for sediments from all sampling locations (PAH abbreviations defined in Table 1).

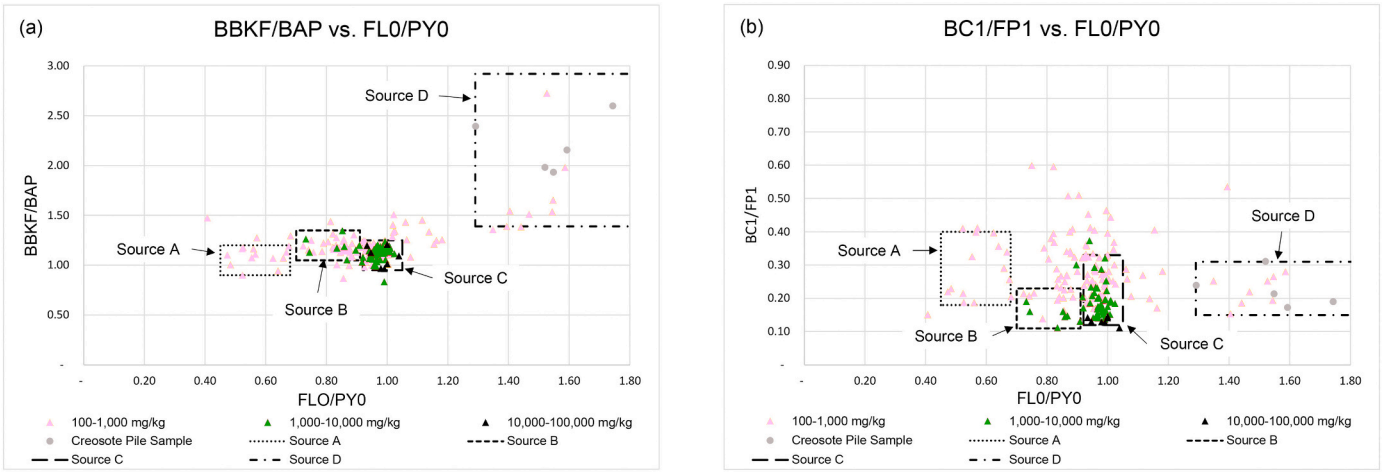

Fig. 3. Select PAH diagnostic ratio cross-plots used as source models for high PAH concentration (TPAH >100 mg/kg) sediments from all sampling locations (PAH abbreviations defined in Table 1).

describes the process of developing the source signatures shown in Fig. 3.

Sediments with relatively high TPAH concentrations that might indicate potential accumulations from significant historical point sources were evaluated to determine the presence of a potential signature (i.e., data cluster). These data clusters for the potential PAH source ratio cross-plots of benzo(b + k)fluoranthene/benzo(*a*)pyrene versus fluoranthene/pyrene (Fig. 3a) and C1-chrysenes/C1-fluoranthenes+pyrenes versus fluoranthene/pyrene (Fig. 3b) were used to define the ranges or boundaries of the plotted PAH diagnostic ratios for these sediments with high TPAH concentrations. Preliminary assessments indicated the potential presence of four distinct signatures, arbitrarily designated as Source A through Source D and correlating to increasing values for the ratio of fluoranthene/pyrene. The signature ranges listed in Table 2 for Source A through Source D were determined by looking at distributions within the sediments with high TPAH concentrations that might represent a potential source or end-member. These ranges in PAH ratio values are site-specific and assigned for the purpose of using these PAH diagnostic source ratios to help differentiate potential sources.

The PAH diagnostic ratio cross-plots (Fig. 3) indicated multiple apparently distinct groupings, with one particularly strong potential signature characterized by relatively high TPAH concentrations and a narrow range for the fluoranthene/pyrene ratio for both ratio pairs. This grouping supported the determination of the signature boundaries for Source C, as ranges for the three PAH diagnostic ratios (Table 2).

The next most prominent potential source signature, designated as Source B, corresponds to the apparent cluster of samples with high TPAH concentrations as shown in Fig. 3, with a generally lower range for fluoranthene/pyrene and boundaries that encompass this data cluster.

Fewer sediment data points defined two other less predominant potential sources, but more definitive signatures, relative to the Source B and Source C signatures, designated as Source A and Source D. The fluoranthene/pyrene ratio range for the Source A signature extends below 0.6. The relatively high fluoranthene/pyrene ratio range for the Source D signature suggested a likely creosote-related source. Studies of sediments containing background PAHs and MGP residues have also identified the presence of creosote, and cross-plots using higher molecular weight PAHs demonstrate a range of about 1.2–1.6 for the fluoranthene/pyrene ratio in creosote (e.g., Costa and Sauer, 2005; McCarthy et al., 2000). Creosote-treated piles from six locations were sampled for PAH analysis (data provided by the Port of San Francisco). These data were used to further define the Source D signature boundaries, and to validate the Source D signature assignments for sediment samples. As shown in Table 2, the fluoranthene/pyrene ratio range for all samples (sediments and creosote pilings) is 1.29–1.97, but only one creosote sample (not shown on Fig. 3) exceeded 1.80. In order to optimize the graphic representations, the figures presented herein show the Source D signature box as truncated but still showing the range for the fluoranthene/pyrene ratio that represents all but the one high-ratio creosote pile sample.

Fig. 4 shows the distributions of the PAH diagnostic ratio-based source assigned samples with TPAH concentrations exceeding 100 mg/kg. Source assignments were based on the signature boundaries shown in Table 2 for sediments at any depth up to greater than 20 ft. below sediment surface. The distributions are shown as approximate lateral extent in surface and subsurface sediment. The impacted sediments extend along the shoreline with subsurface lateral distributions extending outward from the shoreline in two bands following the alignment of historical piers 37 and 41 as shown in Fig. 4. The sediments designated as Source C show the most extensive distributions, with more localized distributions for sediments assigned as Source A, Source B or Source D.

The pyrogenic PAH source types described above are primarily distinguished by differing ranges in the fluoranthene/pyrene ratio, and they are consistent with the expected by-products of three gasification processes used during different time periods at a nearby historical MGP facility. These historical gasification processes would yield lampblack from oil gasification (OG), and different coal tar by-products from the carbureted water gas (CWG) and coal carbonization (CC) processes. The offshore investigation area and adjacent uplands were historically part of San Francisco Bay with tidal mudflats extending from the historical natural shoreline. The upland areas were filled in after a seawall (shown in Fig. 1) was constructed in the late 1800s. Several short piers/wharfs allowed boat access to the shoreline and by 1899, a longer pier, approximately 250 ft long, was constructed. The configurations of the

Table 2
Site-specific assigned ranges for PAH diagnostic source ratios used to differentiate potential pyrogenic point sources.

Signature description	Signature ranges; TPAH > 100 mg/kg[a]		
	FL0/PY0[b]	BBKF/BAP[b]	BC1/FP1[b]
Source A	0.45–0.68	0.90–1.20	0.18–0.40
Source B	0.70–0.91	1.05–1.35	0.11–0.23
Source C	0.92–1.05	0.95–1.25	0.12–0.33
Source D	1.29–1.97	1.39–2.92	0.15–0.31

[a] Total PAH (TPAH) concentration range, based on the RMP PAH list (SFEI, 2016), where source signatures were most distinct.

[b] Observed range for samples above the 100 mg/kg TPAH concentration; FL0/PY0 = fluoranthene/pyrene; BBKF/BAP = benzo(b + k)fluoranthene/benzo(*a*)pyrene; BC1/FP1 = C1-chyrsenes/C1-fluoranthenes+pyrenes.

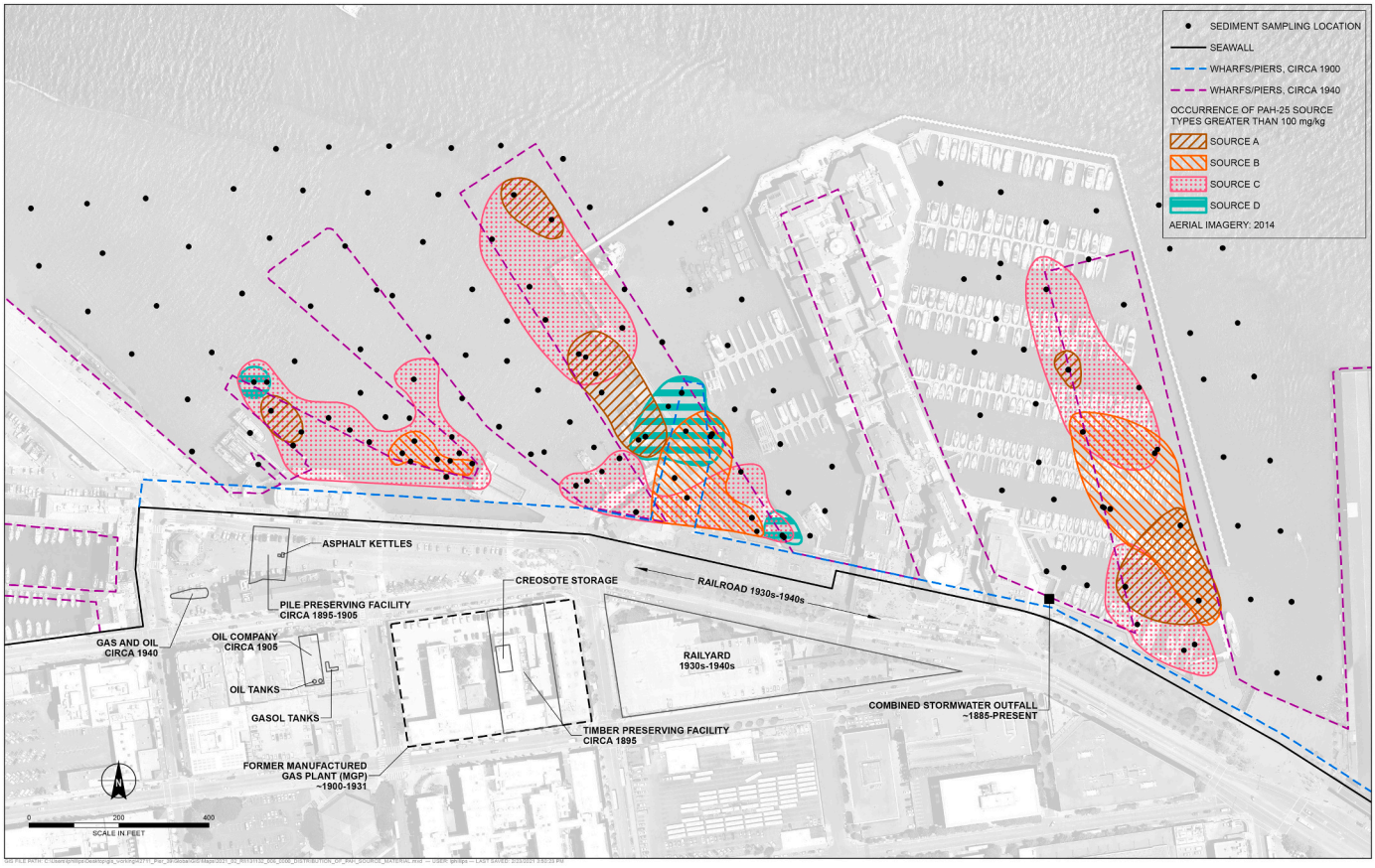

Fig. 4. Inferred PAH diagnostic ratio-based source assignments for sediments with TPAH >100 mg/kg at any depth up to >20 ft. below sediment surface.

piers within the investigation area have changed substantially through time. The four historical rectangular piers shown on Fig. 1 were constructed ~1915, and the more irregular shaped piers to the west were constructed ~1930. The current configuration (aerial photograph in Fig. 1) was primarily constructed in the 1970s and 1980s.

Three known operations that were potential historical sources of PAHs are shown in Fig. 1. Two timber-preserving operations, one using creosote and another using asphalt were operating in the late 1890s. In 1900, the creosoting facility was purchased and converted to a coke and coal manufactured gas production (MGP) facility (Fig. 1). In 1907, gas production was converted from a coal carbonization process to carbureted water gas and oil gas production. In approximately 1931, when natural gas became available, gas manufacturing ceased at this facility. Other potential sources of PAHs include oil facilities that existed to the west of the former MGP as early as 1905, and the railroad and railyard that were in operation in the 1930s and 1940s (Fig. 1). Another potential source of PAHs is a system of combined stormwater sewers conveyed industrial wastes and stormwater runoff directly to the Bay without treatment. The City of San Francisco developed the system in the latter portion of the 19th century and one of the discharge points is within the study area (Fig. 1).

Ranges for the fluoranthene/pyrene ratio from evaluations of former MGP sites across the U.S. have been reported for CWG tars (0.58–0.96) and CC tars (0.86–1.31) (EPRI, 2000; Costa and Sauer, 2005). The OG and CWG processes can produce tars that exhibit fluoranthene/pyrene ratios of about 0.6 (EPRI, 2003). Soils from former MGP facilities contaminated with tars containing significant amounts of lampblack exhibited fluoranthene/pyrene ratios in the approximate range of 0.6–0.9 (Hong and Luthy, 2007). With respect to the fluoranthene/pyrene ratio ranges shown in Table 2, the Source A signature is at the low end of the range for OG and CWG tars, the Source B signature range is within these reported ranges for CWG tars and potentially lampblack, and the Source C signature range is within the reported range for CC tars. The fluoranthene/pyrene ratio range for the Source D signature is in general agreement with reported ranges for other creosote-related sources (EPRI, 2000; Stout et al., 2001; Costa and Sauer, 2005). The creosote presence in investigation area sediments may be attributable to a historical creosoting facility near the former MGP, as well as historical creosote-treated timbers used to construct wharfs and piers in the area (Haley & Aldrich, 2018b).

The results of this first step evaluation indicated that both PAH diagnostic ratio comparisons are valuable as potential source models. Therefore, the evaluations of potential source presence in sediments with lower TPAH concentrations utilized a two-model approach, i.e., two cross-plots, consisting of benzo(b + k)fluoranthene/benzo(*a*)pyrene versus fluoranthene/pyrene and C1-chrysenes/C1-fluoranthenes+pyrenes versus fluoranthene/pyrene. The assignment of a candidate source signature for a particular sediment sample is considered verified when the diagnostic ratios fall within the assigned ranges for all three PAH diagnostic ratios, as shown in Table 2 (i.e., verification by both models). It is recognized that samples not verified by both models may reflect mixing of identified pyrogenic sources with unidentified sources of differing PAH compositions.

3.2. Application of PAH ratio source models to sediment evaluations

The second step of this forensic evaluation applied the source models developed from the sediments with higher TPAH concentrations, and explored the presence of the identified source signatures in sediment samples containing TPAH less than 100 mg/kg for all sampling locations. This step also evaluated the distribution of sediments with TPAH concentrations greater than the current Central San Francisco Bay

ambient concentration (4.5 mg/kg) in the context of being potentially attributable to combined nonpoint and unidentified point sources. The assignment of "urban influence" to such samples was based on the model distributions and lack of two-model verification. However, such assignment does not suggest the absence of some degree of potential influence from and mixing with the high-concentration pyrogenic PAH point sources.

The source model cross-plots applied to the sediments with lower TPAH concentrations (<100 mg/kg) for all sampling locations are shown in Fig. 5. These sediments with lower TPAH concentrations exhibit a distribution where the majority of samples fall outside of the defined signatures (Source A to Source D) for one or both models, and are not confirmed by both models as being predominantly impacted by a specific identified source. These samples are considered related to the presence of "urban influence" throughout the investigation area and may reflect variable extents of mixing with identified sources.

The broad fluoranthene/pyrene ratio range for the predominant cluster of samples falling outside of the source model boundaries in sediments with lower TPAH concentrations is also typical of urban influence where there would be various point and nonpoint PAH sources. The fluoranthene/pyrene ratios for urban-influenced sediments from nine well-studied harbors and waterways on the U.S. East and West coasts have ranged from 0.15 to 1.3, and specifically sediments from Alameda Point, California exhibited ratio values from 0.42 to 1.3 (Stout et al., 2004). Broad ranges in the fluoranthene/pyrene ratios have been noted for other studies describing urban influence with respect to point and nonpoint sources, urban runoff, soils and sediments (Azzolina et al., 2016; EPRI, 2008; Mahler et al., 2005; O'Reilly et al., 2012; Stout et al., 2001; Van Metre et al., 2009). In addition, the general distribution of TPAH concentrations suggests this cluster is unrelated to the model source signatures.

3.3. Multivariate analysis

The third step of the forensic evaluation utilized PVA for data exploration to determine the presence of compositional end-members as expressed with a five end-member model. The PVA-modeled end-members and their relative distributions and mixing proportions can be represented by specific samples with the maximum end-member expressions, as the highest relative percentage of the given end-member. The PVA end-member distributions can be evaluated with t-SNE mapping in terms of TPAH concentration or as gradient maps that show the relative predominance of a given end-member throughout the data population. Fig. 6 shows the PVA t-SNE map of sediment samples for all sampling locations, and the specific samples with the maximum PVA end-member expressions. The end-members are designated as EM1 through EM5, with samples colored to show approximate TPAH concentrations. For example, the pie chart designated as number 1 corresponds to the sample with the maximum expression of end-member 1 (EM1). Other end-members are also present in these maximum end-member expression samples, as indicated by the individual pie charts. The distributions indicate that EM3 is the most significant in samples with the highest TPAH concentrations, and end-members EM1, EM2, EM4, and EM5 are generally associated with lower TPAH concentrations.

Fig. 7 shows the PAH profiles for the samples with maximum end-member expressions shown in Fig. 6. These PAH profiles are considered as representative for a given end-member, based on the compositional similarities to other samples also exhibiting predominance of the given end-member. The PVA-generated PAH profiles for each end-member are shown in Supplemental Fig. S1, where the profiles exhibit the unique PAH compositions that distinguish EM1 through EM5.

The most significant end-member EM3 is represented by the sample with the maximum EM3 expression (Fig. 7c), and this PAH profile is very similar to MGP-related sources such as coal carbonization tars (EPRI, 2000; Stout and Wasielewski, 2004; Uhler and Emsbo-Mattingly, 2006). This sediment sample and others with high TPAH concentrations and similar PAH profiles fall within the PAH diagnostic ratio ranges for both source models that correspond to the Source B or Source C signatures.

EM5 is represented by the sample with maximum EM5 expression (Fig. 7e), that also falls within the PAH diagnostic ratio ranges for both source models that correspond to Source D signatures, confirmed to be creosote-related as previously discussed. The profile of this sediment sample (Fig. 7e) compares to those of highly weathered creosote samples (Brenner et al., 2002; EPRI, 2012), where the naphthalenes and other lower molecular weight PAHs have been depleted. Fig. 7f shows a representative profile for the creosote pile samples that plot near the sediment sample with maximum EM5 expression in Fig. 6. This profile is typical for the creosote pile samples and does not exhibit the extent of weathering with respect to the lower molecular weight PAHs.

EM1 is represented by the sample with the maximum EM1 expression (Fig. 7a). This PAH profile has a pyrogenic character as suggested by the distributions of parent to alkylated PAHs, particularly evident for the fluoranthene/pyrene and chrysene series. The sample profile also shows a relative predominance of benz(*a*)anthracene, chrysene and the higher molecular weight 5–6 ring PAHs. The sample with maximum EM2 expression (Fig. 7b) has a pyrogenic character and shows enrichment of the 5–6 ring PAHs relative to fluoranthene and pyrene. The sample with maximum EM4 expression (Fig. 7d) exhibits a petrogenic character with a distribution similar to a heavier fuel residual material (Uhler et al., 2016), as indicated by the distributions of fluoranthenes/pyrenes, naphthobenzothiophenes, and chrysenes, and their respective

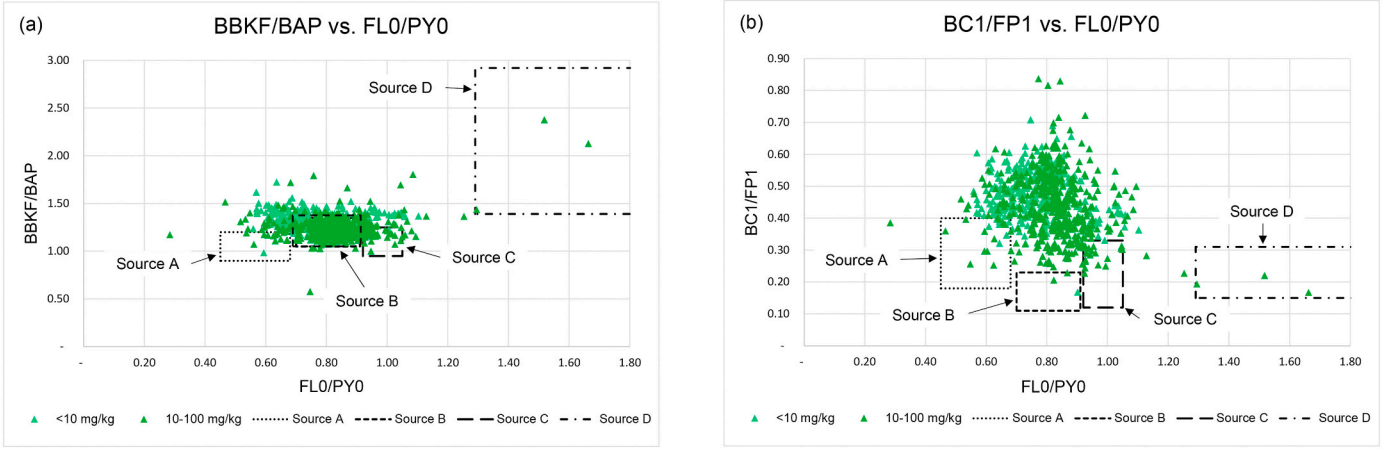

Fig. 5. PAH source models for low PAH concentration (TPAH <100 mg/kg) sediments from all sampling locations (PAH abbreviations defined in Table 1).

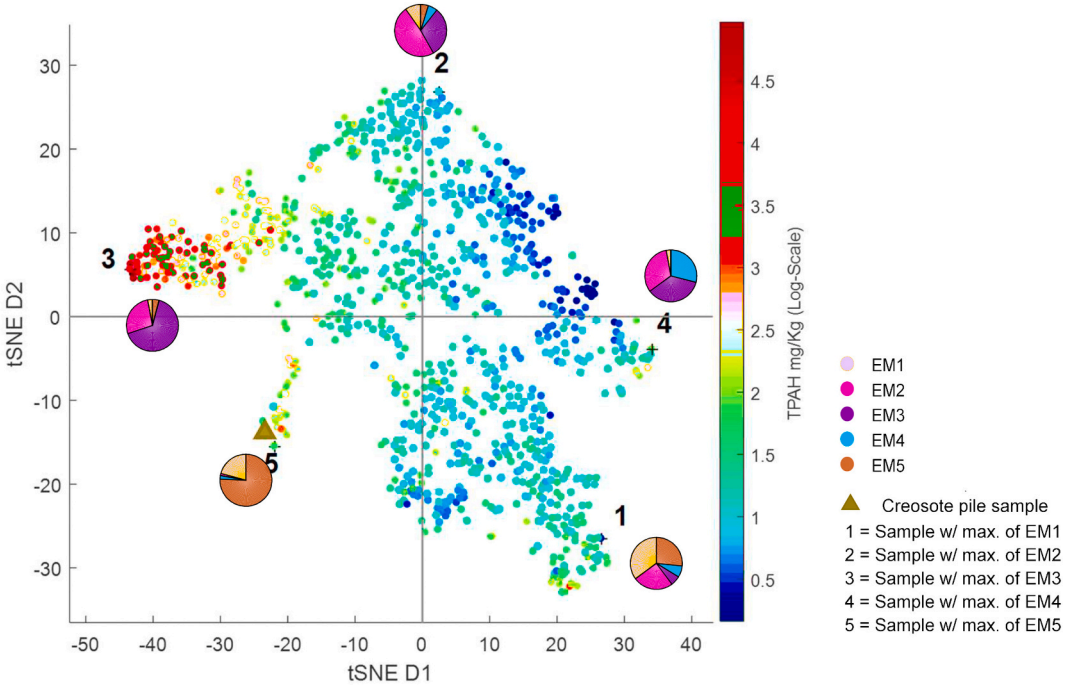

Fig. 6. PVA t-SNE map of sediments from all sampling locations and specific samples with maximum PVA end-member expressions.

alkylated homologues. These specific PAH profiles types (EM1, EM2, and EM4), and other samples with similar PAH profiles, were generally characterized in the PAH diagnostic ratio evaluations to be potentially associated with urban influence.

The relative predominance of the end-members can also be expressed as t-SNE gradient map distributions (see Supplemental for further discussion). In summary, these distributions indicate that EM2 and EM3 are the most predominant end-members with respect to mixing proportions, and that EM2 appears to be more widely distributed throughout the sediment population.

The t-SNE mapping also shows relationships between diagnostic ratio-based sources and end-members, as well as distinctions between the four sources. The PVA t-SNE map in Fig. 8 shows samples that have TPAH concentrations greater than 100 mg/kg and diagnostic ratio-based source assignments (designated as Source A through Source D as previously described by two-model confirmation) and the previously discussed samples with maximum PVA end-member expressions. Fig. 8 also shows source-assigned samples with the maximum (highest) TPAH concentrations (for sources A, B and C). The PAH profiles for these samples are shown in Fig. 9. The Source B and Source C highest TPAH concentration samples cluster near the sample with the maximum EM3 expression (points B, C and 3, respectively, Fig. 8). There is a slight difference between the Source B and Source C highest TPAH concentration samples that are compositionally distinct (e.g., with respect to naphthalene, phenanthrene, and fluoranthene, relative to pyrene), as evidenced by the PAH profiles in Fig. 9. The Source D samples with TPAH >100 mg/kg, the creosote pile samples, and the sample with the maximum EM5 expression all cluster tightly and with a distinct separation from other source-related distributions.

The PVA t-SNE map in Fig. 8 also indicates a potential relationship between Source A, the MGP source-related EM3, the maximum TPAH concentration Source B and Source C samples, and the potentially urban influence-related EM2. The Source A maximum TPAH concentration sample (point A, Fig. 8) is about midway between the EM3 and EM2 maximum expression samples. In between the Source A maximum TPAH concentration sample and the sample with maximum expression of EM2 lie two Source A high TPAH concentration samples (points A' and A", Fig. 8). Also shown are two data points assigned as urban influence by the PAH diagnostic source ratio-based evaluation (points UI' and UI", Fig. 8).

The corresponding PAH profiles show a compositional transition between samples representing Source C and Source B, to Source A, to samples A' and A", to urban influence samples UI' and UI", and to EM2 (Fig. 9a to h, respectively). This transition is characterized by relative changes in the fluoranthene/pyrene ratio and the progressive enrichment of benz(*a*)anthracene, chrysene, and 5–6 ring PAHs, relative to fluoranthene and pyrene. The profile transitions shown in Fig. 9 also correspond to decreasing TPAH concentrations, from source-related samples to urban influence-related samples to the EM2 maximum sample. It is therefore reasonable to assume these transitions are reflect mixing between the potential MGP-related source(s) and the most significant EM2 end-member. The potential higher relative importance of Source A in this mixing may be suggested by both the compositional similarities and decreasing TPAH concentrations between Source A assigned samples, the UI assigned samples and the EM2-related profile (Fig. 9c to h).

3.4. Source evaluation using PVA results and additional PAH ratios

The PVA results provided basis for additional source characterizations through comparison with the previously discussed PAH diagnostic ratio source evaluation. In addition, end-member compositional information was used to evaluate other diagnostic PAHs to further inform source characterization.

A comparison of PAH diagnostic ratio source models with PVA end-member assignments is shown in Fig. 10. End-member assignments for sediment samples were based on the predominance of a particular end-member with a relative abundance above a specified "cut-off" percentage, generally defined as the 95th percentile value for the end-member mixing proportion gradient (Supplemental Figs. S2 through S6). For example, if a sample has a relative EM1 percentage composition greater than 30% (95th percentile value, Fig. S2), and no other end-members are above their respective cut-offs, the sample was assigned as EM1 dominant. For samples with two end-members above cut-off percentages, assignment was based on the largest percentage.

The distributions of PVA end-member assignments within each

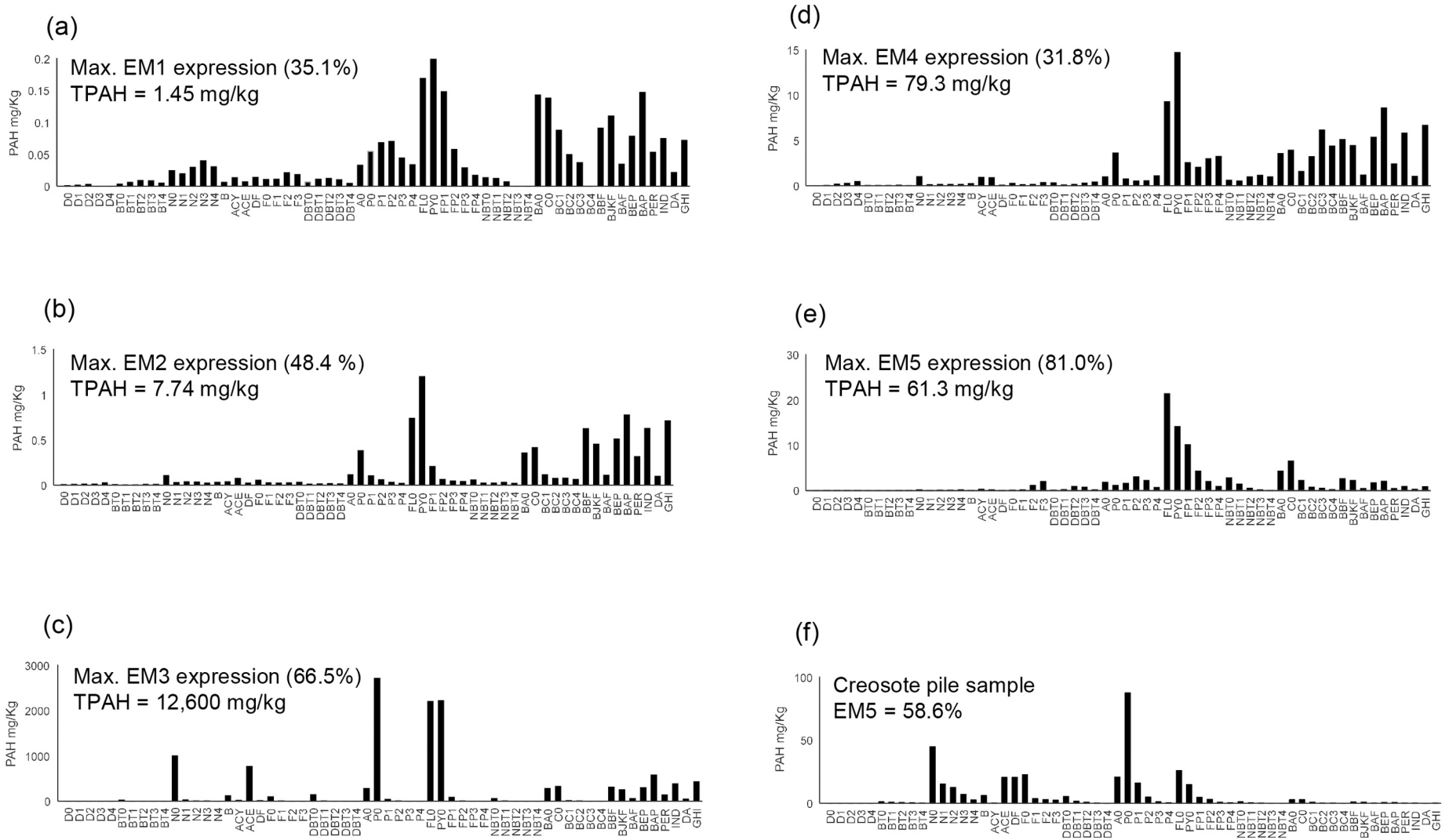

Fig. 7. PAH profiles of (a–e) sediment samples with maximum PVA end-member expressions, and (f) a creosote pile sample (PAH abbreviations defined in Table 1).

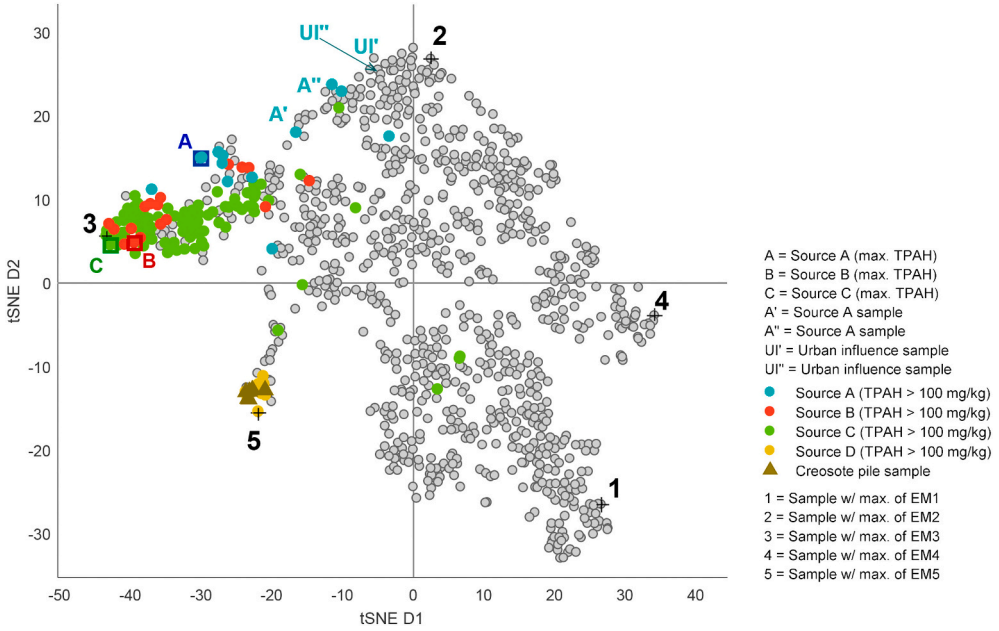

Fig. 8. PVA t-SNE map of sediments from all sampling locations and specific samples with PAH diagnostic ratio-based source assignments and those with maximum PVA end-member expressions.

source model are shown for samples with TPAH >100 mg/kg in Fig. 10a and c. The majority of samples with EM3 dominance fall within the Source C boundaries, but many others fall within the Source B and Source A boundaries. The samples with EM5 dominance largely fall within the Source D boundaries of both models. There are relatively few samples assigned to EM1, EM2, or EM4 that have a TPAH concentration exceeding 100 mg/kg.

The corresponding distributions for the lower concentration samples (TPAH <100 mg/kg) are shown in Fig. 10b and d. These samples with lower TPAH concentrations generally are not assigned to any of the Sources (per required two model confirmation). Most of the samples assigned to EM1, EM2 and EM4 have TPAH <100 mg/kg and do not conform with any of the four Sources. Instead, there is a significant overlap between the cluster of EM1, EM2 and EM4 samples in Fig. 10d and the "urban influence" cluster of samples in the PAH source ratio model shown in Fig. 5b. This suggests a potential correspondence between these ratio-based "urban influence" assignments and end-member compositions EM1, EM2, and EM4. The TPAH concentration ranges for samples assigned as "urban influence" and also assigned to EM1, EM2 or EM4 are 8.55–92.6 mg/kg for EM1, 4.63–77.7 mg/kg for EM2, and 8.75–92.9 mg/kg for EM4. It is acknowledged that samples within these TPAH ranges may contain minor mixtures of PAHs derived from identified pyrogenic sources. These ranges do not include samples with total PAH concentrations lower than ambient (TPAH <4.5 mg/kg) for Central San Francisco Bay sediments, which were excluded from this analysis.

The PAH profiles of samples representing the maximum end-member expressions suggest the potential utility of using select higher-molecular-weight PAH ratios to further characterize both source-related and urban influence signatures. These profiles exhibit compositional differences with respect to benz(*a*)anthracene, chrysene, benzo(b + k)fluoranthene, benzo(*e*)pyrene and benzo(*a*)pyrene. Fig. 11 shows PAH ratio cross-plots using (fluoranthene + pyrene)/(benz(*a*)anthracene + chrysene) versus (fluoranthene + pyrene)/(benzo(b + k)fluoranthene + benzo(*e*)pyrene + benzo(*a*)pyrene). Fig. 11a shows the distribution of the diagnostic ratio Source A, B and C assignments for samples with TPAH >100 mg/kg. The Source A trendline appears to be distinct from the Source B and Source C trendlines, which have similar slopes. The distributions and trendlines for samples assigned to EM2 and EM3 shown in Fig. 11b indicate distinct sample populations (with distinct slopes) between these predominant MGP source-related (EM3) and site-specific pyrogenic background (EM2) end-members. The Source A trendline and the EM2 trendline have essentially the same slope (Fig. 11c) suggesting a potential relationship between Source A and the predominant pyrogenic EM2 that is associated with site-specific background. This is consistent with the evidence presented in Figs. 8 and 9 showing that Source A can be explained as a mixture of EM3 and EM2.

Table 3 summarizes the agreement between the PAH diagnostic ratio-based source assignments and the PVA end-member assignments for the samples with higher concentrations (TPAH >100 mg/kg). For the Source C samples, about 95% were assigned to EM3 (based >45% EM3) or had significant EM3 contributions (34%–45%), and only one sample was assigned to EM2. All Source B samples were assigned to EM3, except one that was a little lower than the 95th percentile criterion. Ten of the 13 of the Source A samples were assigned to EM3 and the other three were assigned to EM2. Source D samples were all assigned to EM5, and five of the six creosote pile samples were assigned to EM5, with 1 sample assigned to EM3 dominant but also having an EM5 percentage exceeding the 95th percentile. For samples identified as urban influence, about 81% were either assigned to EM2 or had significant EM2 percentages. The remaining urban influence samples correspond to lesser degrees with the other end-members.

3.5. Sediment PAH composition in other urban influenced areas

PAHs from multiple sources enter waterways via storm sewer discharges of rainwater and surface water that transport airborne emission particles, road dust, roof and sealant particles, various petroleum products, and other PAH source materials. Urban waterways near large populations, commerce, and industry often include multiple sites and point sources, as well as stormwater and/or combined sewer/stormwater outfalls. The combination of point sources, stormwater discharges, and nonpoint sources of PAHs complicates the task of distinguishing PAHs associated with a specific site/point source from those attributable to "background". Studies documenting "background" PAH concentrations in historical urban sediments (e.g., using depth below sediment surface as a surrogate for time) indicate that concentrations of PAHs in sediments have increased considerably since the early 1900s, and that "background" PAH concentrations are generally

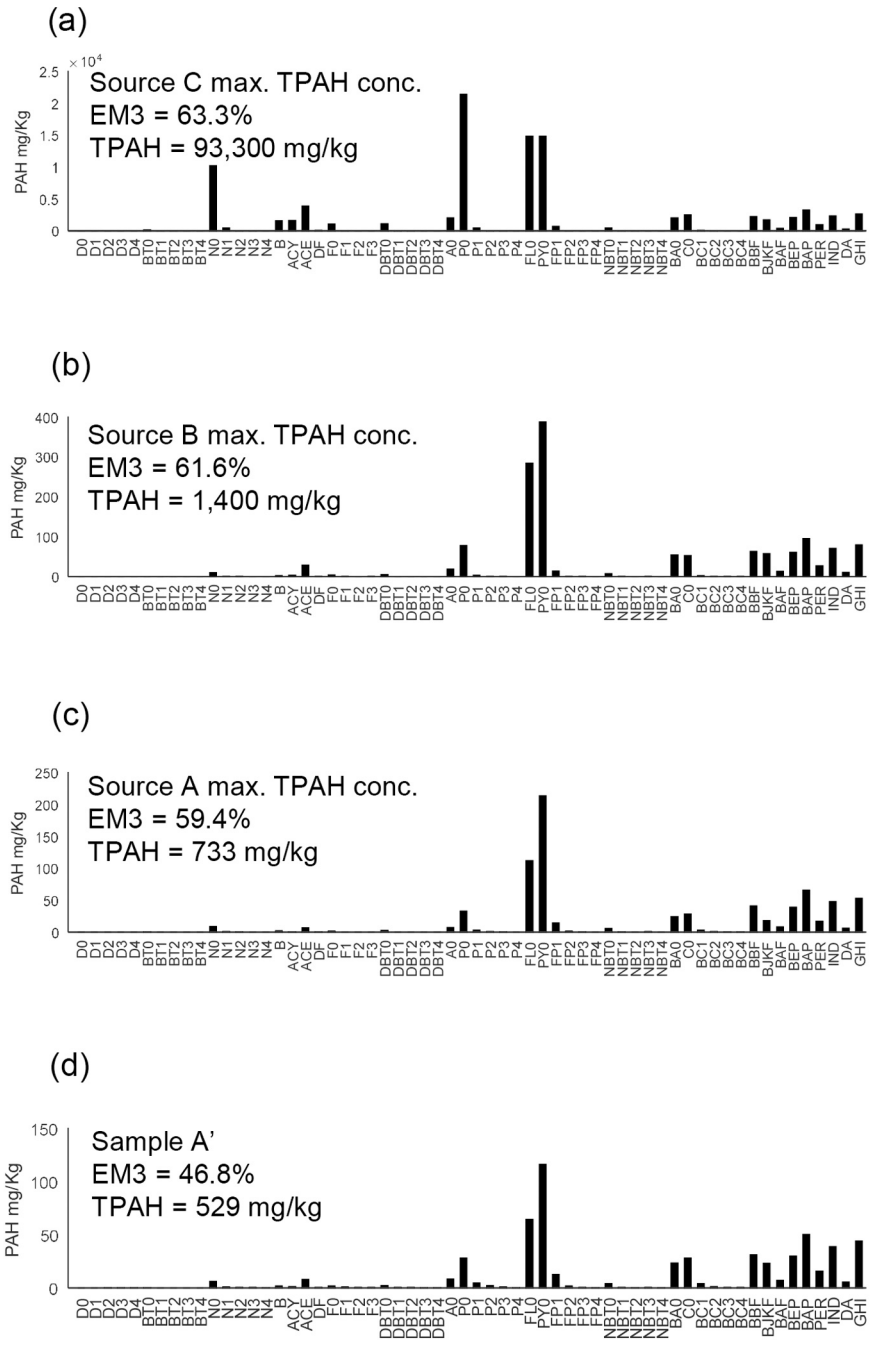

Fig. 9. PAH profiles of (a–e) high TPAH concentration sediment samples with PAH diagnostic ratio-based source assignments, (f–g) samples assigned as urban influence, and (h) sample with maximum PVA end-member EM2 expression (PAH abbreviations defined in Table 1).

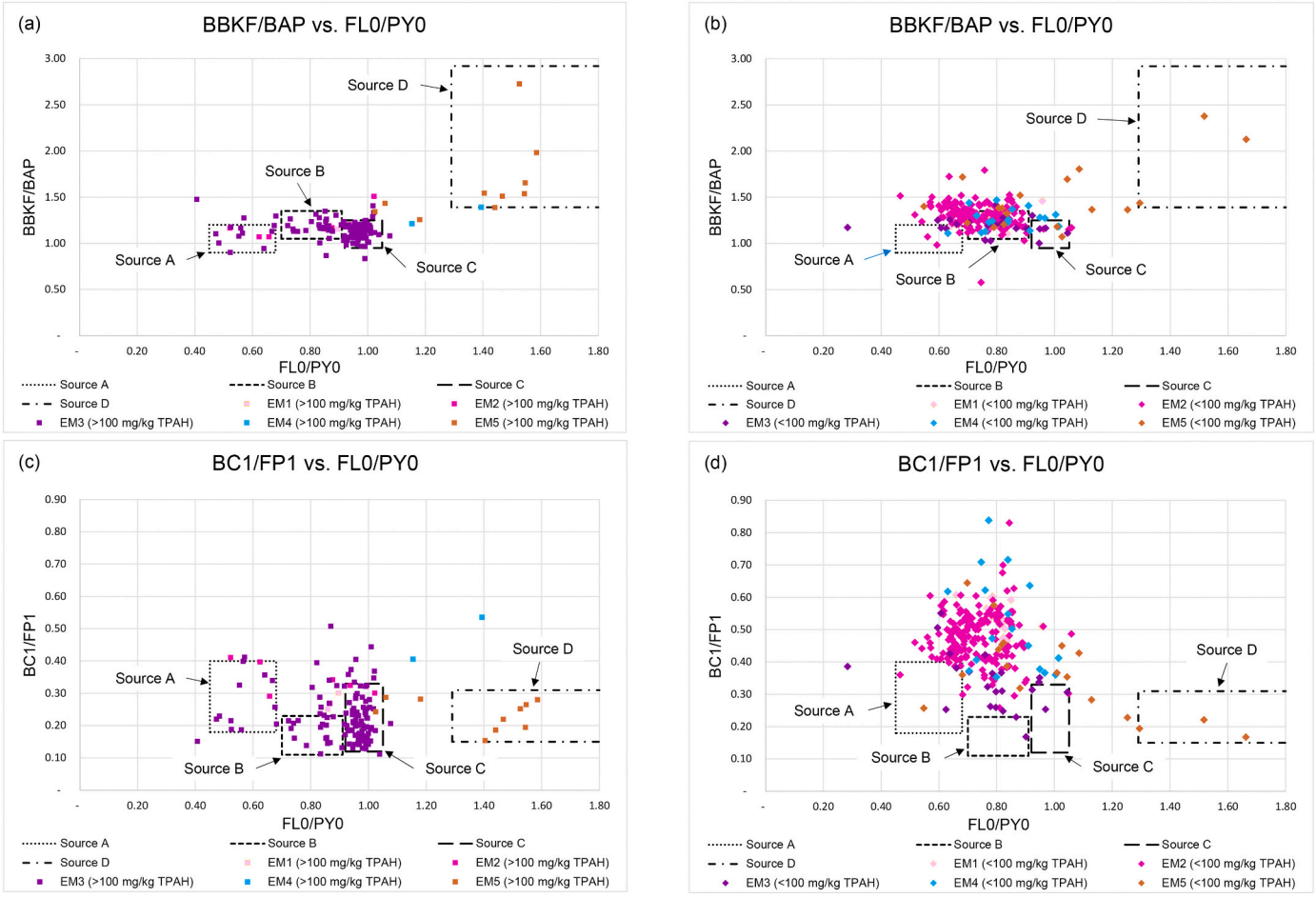

Fig. 10. Distribution of sediment sample PVA end-member assignments relative to the PAH diagnostic ratio source model signatures (PAH abbreviations defined in Table 1).

much higher in inland urban waterways than in coastal bays and estuaries (EPRI, 2000; EPRI, 2012).

The cumulative contributions of these point and nonpoint PAH sources can be significant for urban influenced areas. Total EPA16 (Priority Pollutant PAH) concentrations (defined as "background") in sediments from various U.S. industrialized urban waterways have been shown to range up to 20 mg/kg (Stout et al., 2004). Urban area lakes across the U.S. which were unaffected by any known/suspected waste sites had surface sediment total PAH concentrations between 20 mg/kg and 50 mg/kg, and subsurface sediment total PAH concentrations greater than 200 mg/kg (based on 19 parent PAHs and their alkyl-substituted homologues) have been measured for lakes near highly urbanized areas (Van Metre et al., 2000). For comparison, the total PAH concentration ranges in this study calculated as the sum of EPA's 16 Priority Pollutant PAHs are 7.62–83.7 mg/kg for EM1, 4.10–68.9 mg/kg for EM2, and 7.77–85.4 mg/kg for EM4.

3.6. Potential uncertainties

Although preliminary source assignments can be made for the sediment samples (surface, subsurface), based on PAH biplots in conjunction with other criteria such as geospatial relationships between sample locations, the use of two independent forensic evaluation approaches (PAH diagnostic ratio evaluations and multivariate analysis) enhances the ability to make more confident source assignments. With respect to sediment samples with TPAH concentrations between 4.5 mg/kg and 100 mg/kg, the combined forensic approaches improve the determination of which samples more likely reflect nonpoint and potential unidentified point source urban influence, and which samples more likely reflect some degree of mixing between likely MGP-related sources and urban influence. The t-SNE gradient map for each end-member shows the distribution with respect to mixing proportions, expressed as a composition percentage of the end-member for all sediment samples in Supplemental Figs. S2 through S6.

The distinction between urban influence and point source mixing with urban influence becomes more challenging for sediments with lower TPAH concentrations, and any potential uncertainties with respect to PAH concentrations in the diagnostic ratios used in potential source assignments should be considered. The selected PAH diagnostic ratios used for forensic analysis were selected to be representative of the source material and also show environmental stability, the latter of which has been documented as being suitable for the diagnostic ratios used in this evaluation (Uhler and Emsbo-Mattingly, 2006). With respect to representativeness and assessing possible source influence, the potential for petrogenic contribution to the sediment population of alkylated PAH compounds should be considered for sediments with lower TPAH concentrations. Petrogenic source types such as crude petroleum, heavy fuel oils, lubricating oils, and diesel fuels do contain low concentrations of C1-fluoranthenes+pyrenes and C1-chrysenes, and the relative abundance (i.e., ratios) of these PAHs can vary significantly between these petrogenic source types (Burns et al., 1997; Neff et al., 1998; Uhler et al., 2016). The predominance of pyrogenic PAHs in urban waterway sediments (Stout et al., 2004) also suggests that non-MGP pyrogenic sources may contribute to the distributions of these C1-alkylated PAHs. Any meaningful assessment of potential influence by petrogenic sources for the C1-fluoranthenes+pyrenes to C1-chrysenes

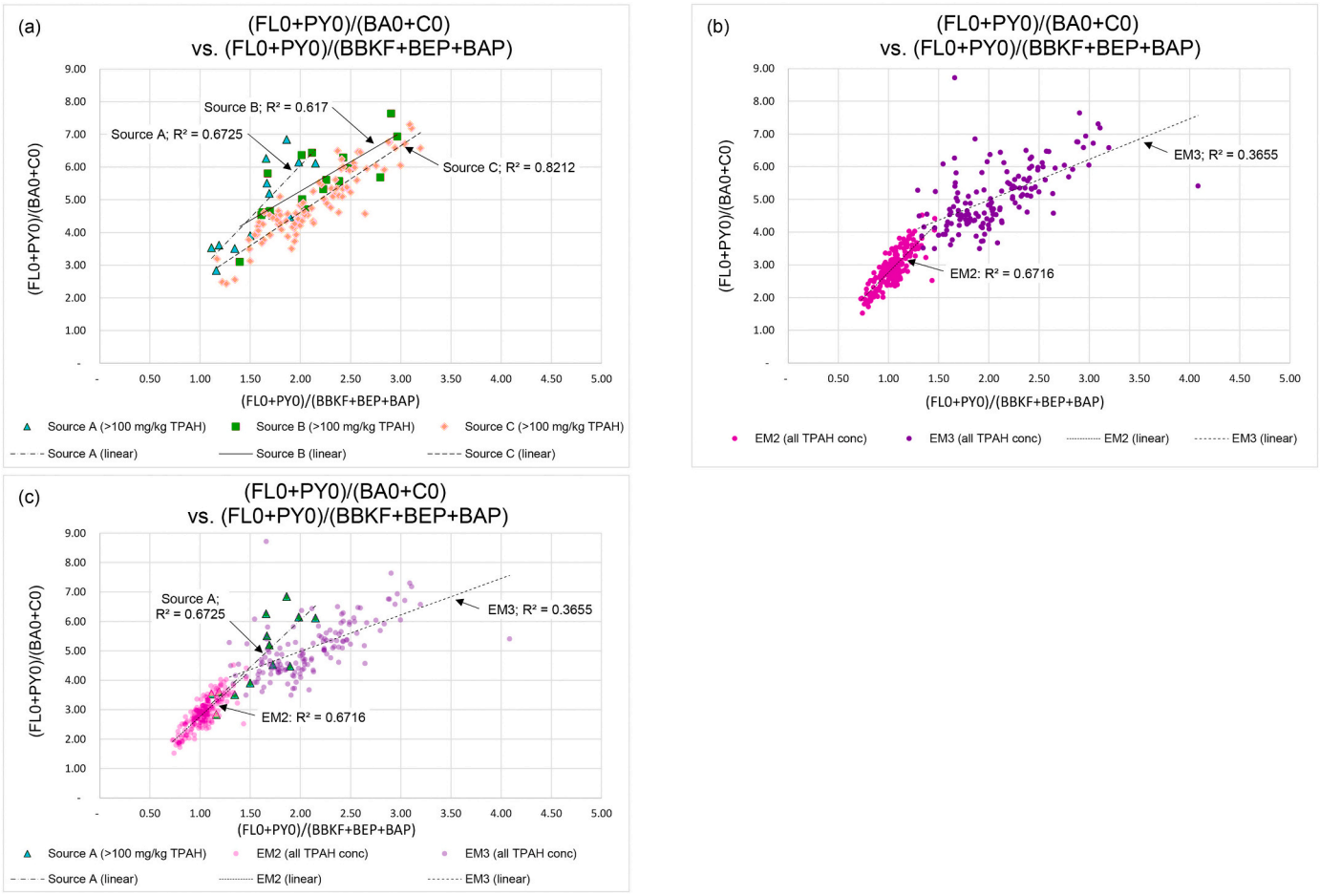

Fig. 11. Select PAH diagnostic ratio cross-plots for sediments with (a) diagnostic ratio Sources A–C assignments, (b) distributions of sediment sample PVA end-member assignments, and (c) correspondence of PVA end-member and Source A assignments (PAH abbreviations defined in Table 1).

Table 3
Agreement between PAH diagnostic ratio-based source assignments and PVA end-member results.

PAH diagnostic ratio assignments			Distribution of end member assignments (based on % end member contribution)									
Designation	TPAH range	Total samples	Dominant PVA end member	EM1		EM2		EM3		EM4	EM5	No assignment[b]
				>30%[a]	20–30%	>40%[a]	30–40%	>45%[a]	35–45%	>12%[a]	>30%[a]	
Source A	>100 mg/kg	13	EM3			3		10				
Source B	>100 mg/kg	17	EM3					16	1			
Source C	>100 mg/kg	88	EM3			1	3	77	7			
Source D	>100 mg/kg	7	EM5								7	
Creosote pile	>2000 mg/kg	6	EM5					1[c]			5	
Urban influence	>4.5 mg/kg	450	EM2	12	3	118	247	4	15	13	7	31

[a] Cut-off for end-member (EM) assignment, based on the 95th percentile value for EM mixing proportion gradient for indicated EM.
[b] Sample in which none of the five end-members are present above the indicated cut-off percentages.
[c] Sample is 49% EM3, but also 40% EM5.

diagnostic ratio will be confounded by the complex nature of urban influence as a mixture of nonpoint and potential unidentified point sources, and the potential contribution from non-MGP pyrogenic sources. However, for the study area in this evaluation the potential for relatively low petrogenic influence in sediments with lower TPAH concentrations is supported by the multivariate analysis component that defined five end-members, with the least significant being of petrogenic character.

4. Conclusions

The forensic evaluations of PAHs in nearshore sediments in San

Francisco Bay support the following observations and conclusions:

- The sediments with higher TPAH concentrations exhibited PAH diagnostic ratio distributions with potentially distinct sample groupings, suggesting the presence of multiple potential point source signatures.
- The PAH diagnostic ratio evaluations identified four potential point source signatures in sediments with higher PAH concentrations. Three signatures show pyrogenic character (Sources A, B and C) likely consistent with historical MGP sources, and one signature (Source D) was verified as being related to creosote through the forensic evaluation of samples taken from creosote-treated piles.
- An additional source category of PAHs to investigation area sediment consists of ubiquitous nonpoint and potential unidentified point sources, which is distinguished from the four identified point source signatures. This additional source category is termed "urban influence".
- A multivariate analysis using PVA and t-SNE for data evaluation defined two end-members related to pyrogenic sources and three end-members potentially related to urban influence. One end-member (EM3) corresponds to the two most significant MGP-related source signatures identified by PAH diagnostic ratio analysis, designated as Source B and Source C. A second end-member (EM5) corresponds to the creosote-related Source D signature and associated sediment samples. Three end-members (EM1, EM2 and EM4) are primarily associated with sediments with lower total PAH concentrations and correspond to the urban influence source category identified by the diagnostic ratio approach. Two of these end-members (EM1, EM2) are pyrogenic and the least significant is of petrogenic nature (EM4).
- The PVA analysis results suggested that the third potential "MGP-related" PAH source signature (Source A) may be related to mixing of higher concentration MGP-related sources (Sources B and C) and the most widely distributed end-member that is related to urban influence, as evidenced by the t-SNE mapping distributions of the Source A signature and the associated end-members.
- The PVA analysis was unable to effectively resolve Sources B and C, identified through the cross-plot source models, both of which are suspected distinct MGP-related sources based on known historical operations of the former MGP. This outcome illustrates the complementary utility of multiple tools in addressing project-specific forensic objectives.
- The PVA results suggested the utility of other high-molecular-weight PAH diagnostic ratios for further characterization of source-related and urban influences. Select PAH diagnostic ratio distributions suggested potential distinctions between Source A and the more significant MGP-related sources (Sources B and C). The selected PAH diagnostic ratio distributions with respect to end-member assignments and associated trendlines further supported the distinction between the predominant end-member associated with source-related influences from the predominant end-member related to urban influence.
- Urban influence is understood to occur throughout the entire investigation area, and therefore, where the PAH contribution a candidate point source predominates, it is inferred that the point source influence masks the urban influence. Sediment samples with PAH compositional characteristics suggesting a mixture of potentially MGP-related sources and urban influence, this mixing is understood to occur where point source impacts intermingle with the ubiquitous urban influence (recognizing that urban influence includes nonpoint sources and also unidentified point-source PAHs, which also occur in urban waterways).

Supplementary data to this article can be found online at https://doi.org/10.1016/j.marpolbul.2021.112248.

CRediT authorship contribution statement

Randy E. Jordan: Conceptualization, Methodology, Validation, Formal analysis, Investigation, Resources, Writing – original draft, Writing – review & editing, Visualization, Supervision, Project administration. **Mark J. Cejas:** Conceptualization, Methodology, Software, Validation, Formal analysis, Investigation, Resources, Writing – original draft, Visualization. **Helder J. Costa:** Conceptualization, Methodology, Validation, Formal analysis, Investigation, Resources, Writing – original draft, Writing – review & editing, Visualization, Supervision, Project administration, Funding acquisition. **Theodor C. Sauer:** Methodology, Formal analysis, Investigation, Writing – review & editing. **Laura S. McWilliams:** Conceptualization, Methodology, Validation, Formal analysis, Investigation, Resources, Data curation, Writing – review & editing, Visualization, Supervision.

Declaration of competing interest

The authors declare that they have no known competing financial interests or personal relationships that could have appeared to influence the work reported in this paper.

Acknowledgements

The authors would like to thank the Port of San Francisco and NewFields for providing data from creosote-treated pile samples. This work was sponsored by PG&E through a consulting agreement with Haley & Aldrich, Inc. The findings were vetted with the Port of San Francisco and the California Regional Water Quality Control Board, the lead regulatory agency.

References

Azzolina, A.A., Kreitinger, J.P., Skorobogatov, Y., Shaw, R.K., 2016. Background concentrations of PAHs and metals in surface and subsurface soils collected throughout Manhattan, New York. Environ. Forensic 17 (4), 294–310. https://doi.org/10.1080/15275922.2016.1230905.

Boehm, P.D., Pietari, J., Cook, L.L., Saba, T., 2018. Improving rigor in polycyclic aromatic hydrocarbon source fingerprinting. Environ. Forensic 19 (3), 172–184. https://doi.org/10.1080/15275922.2018.1474287.

Brenner, R.C., Magar, V.S., Ickes, J.A., Abbott, J.E., Stout, S.A., Crecelius, E.A., Bingler, L. S., 2002. Characterization and fate of PAH-contaminated sediments at the Wyckoff/Eagle Harbor superfund site. Environmental Science & Technology 36 (12), 2605–2613. https://doi.org/10.1021/es011406u.

Burns, W.A., Mankiewicz, P.J., Bence, A.E., Page, D.S., Parker, K.R., 1997. A principal-component and least-squares method for allocating polycyclic aromatic hydrocarbons in sediment to multiple sources. Environ. Toxicol. Chem. 16 (6), 1119–1131.

Cejas, M.J., Barrick, R., 2021. Chemometric mapping of polychlorinated dibenzo-p-dioxin (PCDD) and dibenzofuran (PCDF) congeners from the Passaic River, NJ: integrated application of RSIMCA, PVA and t-SNE. Environ. Forensic 22 (1–2), 155–171. https://doi.org/10.1080/15275922.2020.1834022.

Costa, H.J., Sauer, T.C., 2005. Forensic approaches and considerations in identifying PAH background. Environ. Forensic 6 (1), 9–16. https://doi.org/10.1080/15275920590913859.

Costa, H.J., White, K.A., Ruspantini, J.J., 2004. Distinguishing PAH and MGP residues in sediments of a freshwater creek. Environ. Forensic 5 (3), 171–182. https://doi.org/10.1080/15275920490495909.

Douglas, G.S., Bence, A.E., Prince, R.C., McMillen, S.J., Butler, E.L., 1996. Environmental stability of selected petroleum hydrocarbon source and weathering ratios. Environmental Science & Technology 30 (7), 2332–2339.

Ehrlich, R., Wenning, R.J., Johnson, G.W., Su, S.H., Paustenbach, D.J., 1994. A mixing model for polychlorinated dibenzo-*p*-dioxins and dibenzofurans in surface sediments from Newark Bay, New Jersey using Polytopic vector analysis. Arch. Environ. Contam. Toxicol. 27, 486–500. https://doi.org/10.1007/BF00214840.

Electric Power Research Institute (EPRI), 2000. Chemical Source Attribution at Former MPG Sites. Prepared by META Environmental. EPRI, Palo Alto, CA, NYSEG, Binghamton, NY, and RG&E, Rochester, NY. Report 1000728.

EPRI, 2000. Literature Review of Background Polycyclic Aromatic Hydrocarbons. Prepared by META Environmental. EPRI, Palo Alto, CA. Report TR-114755.

EPRI, 2003. Identifying PAHs from Manufactured Gas Plant Sites. Prepared by Battelle Memorial Institute. EPRI, Palo Alto, CA. Report 1005289.

EPRI, 2008. Examination of the Sources of Polycyclic Aromatic Hydrocarbon (PAH) in Urban Background Soil. Prepared by META Environmental. EPRI, Palo Alto, CA, NYSEG, Binghamton, NY, and RG&E, Rochester, NY. Interim Report 1015558, December.

EPRI, 2012. Determining PAH Background in Sediments. Prepared by Haley & Aldrich, Inc. EPRI, Palo Alto, CA. Report 1023744.

Full, W.E., Ehrlich, R., Klovan, J.E., 1981. EXTENDED QMODEL -objective definition of external end-members in the analysis of mixtures. Math. Geol. 13, 331–344. https://doi.org/10.1007/BF01031518.

Haley & Aldrich, 2018a. Data Gap Report, Pier 39 to Pier 45 Investigation, San Francisco, California. 6 July. GeoTracker ID: T1000007367.

Haley & Aldrich, 2018b. Remedial Investigation Report, Pier 39 to Pier 45 Sediment Investigation, San Francisco, California. 21 December. GeoTracker ID: T1000007367.

Haley & Aldrich, Inc. (Haley & Aldrich), 2017. Sediment Characterization Report, Pier 39 to Pier 45 Investigation, San Francisco, California. 27 October. GeoTracker ID: T1000007367.

Hong, L., Luthy, R.G., 2007. Availability of polycyclic aromatic hydrocarbons from lampblack-impacted soils at former oil-gas plant sites in California, USA. Environ. Toxicol. Chem. 26 (3), 394–405.

Mahler, B.J., Van Metre, P.C., Bashara, T.J., Wilson, J.T., Johns, D.A., 2005. Parking lot sealcoat: an unrecognized source of urban polycyclic aromatic hydrocarbons. Environmental Science & Technology 39, 5560–5566. https://doi.org/10.1021/es0501565.

McCarthy, K.J., Emsbo-Mattingly, S.D., Stout, S.A., Uhler, A.D., 2000. Identifying Manufactured Gas Plant Residues in Industrial Sediments. Soil, Sediment Groundwater October/November:1–3.

Miesch, A.T., 1976. Q-mode Factor Analysis of Geochemical and Petrologic Data Matrices With Constant Row-sums. No. 574-G. U.S. Government Printing Office, 54 pp.

Neff, J.M., Ostazeski, S.A., Macomber, S.C., Roberts, L.G., Gardiner, W., Word, J.Q., 1998. Weathering, Chemical Composition and Toxicity of Four Western Australian Crude Oils. Report to Apache Energy Ltd., Perth, Western Australia, Australia.

NewFields, 2015. Pier 39 PAH Fingerprinting Study Data Report. Prepared for Port of San Francisco, CA. June. GeoTracker ID: T1000007367.

O'Reilly, K., Pietari, J., Boehm, P., 2012. Forensic assessment of refined tar-based sealers as a source of polycyclic aromatic hydrocarbons (PAHs) in urban sediments. Environ. Forensic 13, 185–196. https://doi.org/10.1080/15275922.2012.676598.

San Francisco Estuary Institute (SFEI), 2016. Updated Ambient Concentrations of Toxic Chemicals in San Francisco Bay Area Sediments. Technical Memorandum. February 26.

Stout, S.A., Wasielewski, T.N., 2004. Historical and chemical assessment of the sources of PAHs in soils at a former coal-burning power plan, New Haven, Connecticut. Environ. Forensic 5, 195–211. https://doi.org/10.1080/15275920490886789.

Stout, S.A., Magar, V.S., Uhler, R.M., Ickes, J., Abbott, J., Brenner, R., 2001. Characterization of naturally-occurring and anthropogenic PAHs in urban sediments-Wycoff/Eagle Harbor superfund site. Environ. Forensic 2, 287–300. https://doi.org/10.1006/enfo.2001.0057.

Stout, S.A., Uhler, A.D., Embso-Mattingly, S.D., 2004. Comparative evaluation of background anthropogenic hydrocarbons in surficial sediments from nine urban waterways. Environmental Science & Technology 38 (11), 2987–2994. https://doi.org/10.1021/es040327q.

Uhler, A.D., Emsbo-Mattingly, S.D., 2006. Environmental stability of PAH source indices in pyrogenic tars. Bull. Environ. Contam. Toxicol. 76, 689–696. https://doi.org/10.1007/s00128-006-0975-1.

Uhler, A.D., Stout, S.A., Douglas, G.S., 2016. Chemical character of marine heavy fuel oils and lubricants. In: Stout, S.A., Wang, Z. (Eds.), Standard Handbook Oil Spill Environmental Forensics, Fingerprinting and Source Identification. Academic Press, Second Edition.

van der Maaten, L.J.P., Hinton, G., 2008. Visualizing data using t-SNE. J. Mach. Learn. Res. 9 (11), 2579–2605.

Van Metre, P.C., Mahler, B.J., Furlong, E.T., 2000. Urban sprawl leaves its PAH signature. Environmental Science & Technology 34, 4064–4070. https://doi.org/10.1021/es991007n.

Van Metre, P.C., Mahler, B.J., Wilson, J.T., 2009. PAHs underfoot: contaminated dust from coal-tar sealcoated pavement is widespread in the United States. Environmental Science & Technology 43 (1), 20–25. https://doi.org/10.1021/es802119h.

Yunker, M.B., Macdonald, R.W., Vingarzan, R., Mitchell, R.H., Goyette, D., Sylestre, S., 2002. PAHs in the Frasier River basin: a critical appraisal of PAH ratios as indicators of PAH source and composition. Org. Geochem. 33, 489–515. https://doi.org/10.1016/S0146-6380(02)00002-5.